33rd Annual International Conference of the IEEE EMBS
Boston, Massachusetts USA, August 30 - September 3, 2011

Three-Dimensional Mapping of Strain in *Ex Vivo* Porcine Cornea with an Ultrasound Elasticity Microscope

Kyle W. Hollman, *Member, IEEE,* Sakya Tripathy, and Kang Kim, *Member, IEEE*

***Abstract*—High frequency strain mapping of a porcine cornea was produced by three-dimensional speckle tracking of a three-dimensional confocally merged ultrasonic data set. Previous two-dimensional elasticity imaging was limited by speckle moving in the non-imaged dimension. This study used an ultrasonic transducer (53 MHz center frequency, 31 MHz bandwidth, 1.67 f#) scanned in three dimensions. A fresh porcine eye globe was embedded in gelatin up to the cornea/sclera junction and pressurized to physiological pressure. A portion of the cornea was imaged with a single element transducer scanned in three directions. Three-dimensional volume sets were created from the data by confocally merging volume sets at several depths. In the vertical dimension, parallel to ultrasonic propagation, the transducer was moved by nearly half its depth of field. Overlaps between adjacent depths were correlated using phase-sensitive speckle tracking to determine precise shifts. Two-dimensional images over multiple depths of field were combined to form a single 2-D image over an entire vertical scan range. Multiple planes were then stacked in the remaining direction to form a 3-D volume set. Next, the cornea was deformed and then imaged again. Three-dimensional speckle tracking was used to create strain maps from the two volume sets. Vertical strain, horizontal strain, and transverse strain behave as expected and provide insight into mechanical properties of corneal tissue.**

I. Introduction

ULTRASOUND elasticity imaging is a valuable noninvasive tool to investigate mechanical characteristics of biological tissue [1-5]. It relies on accurate estimates of tissue motion between two frames before and after tissue deformation. Speckle tracking was initially introduced in one dimension to estimate motion along the axial direction (the beam propagation direction) [2,4] and has been expanded into two dimensions with the development of current 2-D ultrasound imaging systems. 2-D speckle tracking measures displacements of a speckle pattern in both axial and lateral (perpendicular to the beam direction in the imaging plane) dimensions [6-10]. The most commonly used elasticity imaging techniques are based on 2-D correlation-based speckle tracking methods [7-10]. Speckle displacements are estimated from correlation lags corresponding to the maximum correlation coefficient between the frames.

Unfortunately, tissue deformations do not necessarily respect the limited dimensionality of 2-D tracking. Large systematic errors can occur when tissue moves perpendicular to the imaging plane. Even when deformation is controlled by researchers, limitations on tissue motion can hamper gathering complete and proper data sets. Therefore, with better computational speed and power, as conventional ultrasound imaging expands into three dimensions [11-13] it is natural for elasticity imaging to follow.

The advantages of 3-D elasticity imaging at lower clinical frequencies should also apply to higher frequency (>50 MHz) imaging with applications in particular to ophthalmic imaging. The eventual clinical goal for high frequency ultrasonic elasticity imaging as examined in this study is keratoconus, affecting about 1 in 2,000 Americans [14]. Because it results as breakdown in corneal elasticity, measurements of mechanical properties may help detect this disease before symptoms become noticeable. This technique could also help guide corneal transplant surgery for advanced cases. Additionally, some less prevalent diseases also affect the elasticity of the cornea including kertoglobus and other corneal dystrophies. As another secondary benefit, corneal elasticity mapping might be useful in guiding improved corneal refractive surgery. It also has potential for assessing the long-term affects of LASIK.

II. Methods

A. Equipment

Although there have been recent advances in technology, ultrasonic transducer arrays at frequencies of 50 MHz or higher are still quite practical for 3-D elasticity measurements. Therefore, for this study, a single element high-frequency transducer was used. The custom-built LiNbO transducer has a center frequency of 53 MHz and bandwidth of 31 MHz. It is tightly focused as indicated by an f-number of 1.67 and a focal length of 4.18 mm. Its axial resolution is 23.9 μm, its lateral resolution is 46.6 μm, and its depth of field is 311 μm.

The electrical setup is very similar to the original 2-D elasticity microscope [15-17]. An excitation signal

Manuscript received March 25, 2011. This work was supported in part by a grant from the National Institute of Health, EY018727, and a NIH center core (P30) grant, EY007003.

K. W. Hollman, was with the University of Michigan, Ann Arbor, MI 48109 USA. He is now with Sound Sight Research, LLC, Livonia, MI 48152 USA (e-mail: kyle.hollman@soundsightresearch.com).

S. Tripathy was with the University of Pittsburgh and UPMC, Center for Ultrasound Molecular Imaging and Therapeutics and Cardiovascular Institute, Pittsburgh, PA. He is now with Simulia, Cleveland, OH.

K. Kim is with the University of Pittsburgh and UPMC, Center for Ultrasound Molecular Imaging and Therapeutics, Cardiovascular Institute, and Bioengineering Department, Pittsburgh, PA 15213 USA (e-mail: kangkim@pitt.edu).

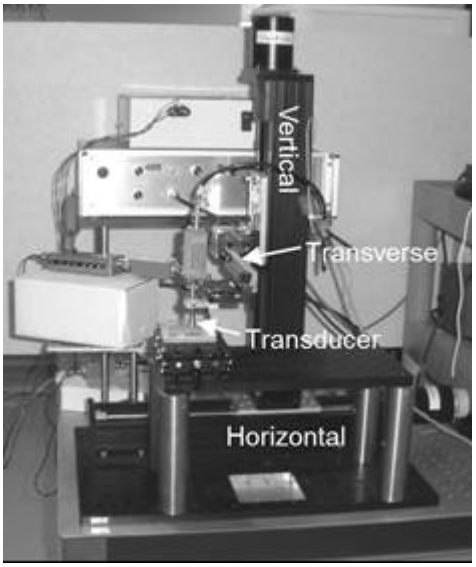

Figure 1. Photograph of setup. Transducer is attached to the transverse axis through a manually controlled tilt stage.

originates in a broadband, high-frequency pulser. From there it travels through a diode expander to reduce baseline noise and into the transducer where it is converted into ultrasonic waves. Signals received by the transducer go into a diode limiter which blocks some of the high amplitude excitation signal from the receiving electronics. The received signal is amplified by two pairs of push-button attenuators and 32 dB fixed-gain amplifiers. Finally, the signal is captured by a high-speed 8-bit digitizing board. For these experiments signals where sampled at a rate of 250 MHz. Using a custom-built circuit, a 10 MHz synchronized output from the digitizing board was divided down to a 9.76 kHz square wave that was used to trigger both pulser and digitizing board. Synchronization helps to reduce signal to signal jitter and therefore improves the efficiency of signal averaging. Three-dimensional images were created from captured raw signals by first confocally merging 2-D images in the vertical/transverse plane and then stacking the planes in the horizontal direction.

As shown in Fig. 1, the transducer is positioned by a three axes stepper motor system. For axes are labeled as 'vertical', 'horizontal', and 'transverse'. The transducer is attached to the transverse axis through a tilt stage to allow for alignment. Each axis is a stepper motor driven screw drive. The vertical axis moves in the direction of ultrasonic propagation, i.e. the direction the transducer is pointed also known as the axial direction. The horizontal and transverse axes move perpendicular to the vertical axis and each other. This is also known as the lateral direction with respect to the transducer. Because it is cylindrically symmetric, the ultrasonic field produced by the transducer is indistinguishable in any direction perpendicular to the axial direction. Therefore the 'horizontal' and 'transverse' labels are arbitrary but useful for keeping track of the dimensions in the signal processing procedure.

Mechanical deformation was applied to specimens with a 25 mm square aluminum plate that has a 2 mm wide slit machined in it. The deformation plate was positioned with a stepper-motor driven screw axis similar to the positioning axes for the transducer. It is attached at a right angle to an aluminum arm that is bolted to the positioning stage of the axis. In length the slit is slightly shorter than the size of the plate. In earlier experiments with 2D imaging, scanning was done across the width of the slit for 1 mm in the center in order to avoid side lobe reflections from metal edges of the slit. This arrangement mechanically reduced artifacts due to out-of-plane tissue deformation. Adjacent tissue constrains out-of-plane motion along the slit length. Along the slit width, there is a discontinuity of force at the edge that creates both axial and lateral deformation in this plane. With the improvement of 3-D imaging, out-of-plane motion is no longer an issue so deformation can be imaged along the entire length of the slit. Because of practical reasons due to scanning time, current scans have been conducted only over a 1 mm lateral square. With current equipment designed for ex-vivo laboratory measurements scanning time for one volume set is about 24 minutes. Faster scanning axes and the future availability of high frequency arrays should reduce scan rates to clinically acceptable levels.

B. Procedure

A whole porcine eye globe was obtained from a medical research supplier. After harvesting the eye, it was packed in ice and sent via overnight shipping. Upon arrival the eye globe was embedded in gelatin up to the corneal/scleral junction. Once the gelatin set, the specimen was ready for measurement. The rest of the container was then filled with a special ultrasonic coupling fluid designed to inhibit corneal edema. The fluid consists of a water solution of 25% glycerol and 10% dextran-40. This technique has been shown [18] to stabilize the cornea which would otherwise rapidly swell due to edema.

Physiological pressure (15.5 mm Hg) was maintained in the eye globe by inserting a needle into the sclera just below the cornea/sclera junction. The needle is connected to a fluid reservoir by a tube. Pressure is controlled by moving the reservoir up and down. The difference between the height of the cornea and the height of the reservoir surface determines pressure. Pressure was checked by replacing the needle with a monometer at the same position as the cornea.

Prior to scanning, the deformation plate was positioned to be just in contact with the cornea. Next the ultrasonic transducer was scanned in three directions. Scans were 45 sampling sites by 45 sampling sites in the horizontal and transverse directions with 20 μm spacing and 10 sites vertically with 200 μm spacing. After scanning, the deformation plate was moved by 31.75 μm and the specimen was rescanned over the same volume. Signals from the two scans were processed by confocal merging to create two 3-D

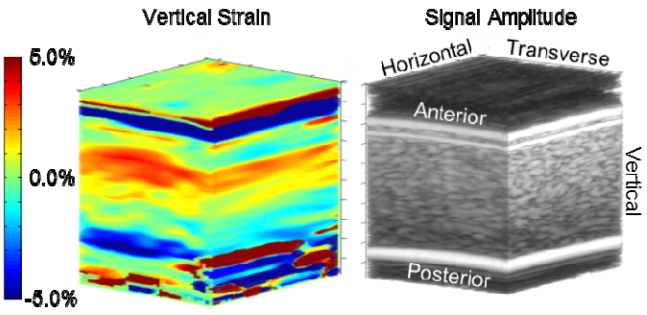

Figure 2. 3D map of strain in the vertical direction for porcine cornea. On the right is a standard 3D image of the signal amplitude displayed over a range of 50 dB.

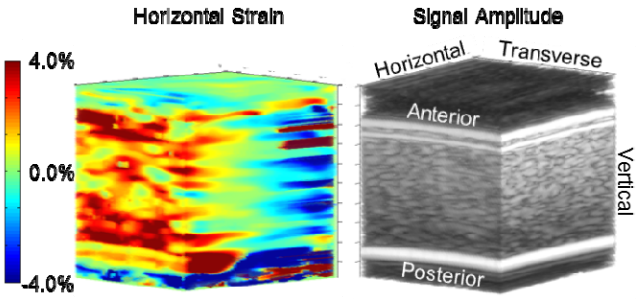

Figure 3. 3D map of strain in the horizontal direction for porcine cornea. On the right is the same standard ultrasonic image as shown in Fig.2.

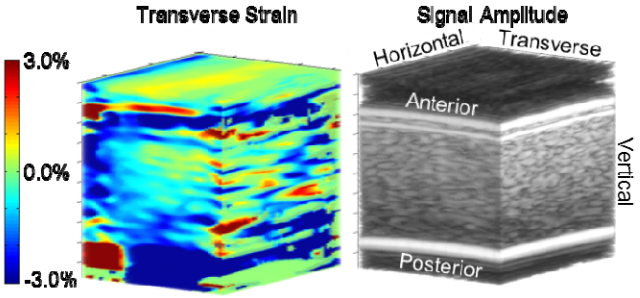

Figure 4. 3D map of strain in the transverse direction for porcine cornea. On the right is the same standard ultrasonic image as shown in Fig.2.

backscatter signal volumes. Confocal merging was similar to 2-D merging described in earlier papers [15, 16]. Finally, 3-D speckle tracking [11-13] was used to determine displacements between the image volumes and then strains were calculated from the displacements in each direction of deformation. For speckle tracking the 3-D kernel measured 75X75X75 μm and the search volume was 25X25X100 μm (horizontal, transverse, vertical).

III. Results

Fig. 2 shows the 3D map of strain in the vertical direction (which also can be referred to as axial strain). On the right is a standard ultrasonic signal amplitude image displayed in a logarithmic (dB) scale. This same image is included in all three figures to show specimen geometry. The two bright white lines at the anterior are the boundaries of the epithelial layer. Above the top boundary is noise from water. The bright line near the posterior is the thin endothelial layer. Between these layers is the stroma, a generally homogenous media made up of layers of crisscrossing collagen fibers. The stromal layers are parallel to the horizontal/transverse plane and stack in the vertical direction. The dimensions of all images are 0.9 mm in both horizontal and transverse directions and 1.4 mm in the vertical direction.

As expected, the vertical strain map in Fig. 2 has mostly features along the vertical direction. In the stroma strain begins with a high positive value near the anterior and gradually shifts toward a high negative value near the posterior. This behavior is consistent with the applied axial deformation force. Note that strain in the interior of the epithelium is mostly green indicating nearly zero strain. This result suggests that the epithelium may be stiffer than the stroma because the deformation is transferred through the epithelium into the stroma with little effect on the epithelium itself.

Fig. 3 offers some of the most convincing evidence that the system is working and the analysis is properly tracking deformation and strain. Remember that the length of the slit is in the transverse direction and its width is in the horizontal direction. The generally axial force being applied by the slit causes a slight pinching in the horizontal direction. In other words, there is a shearing force at each slit edge occurring in the horizontal/vertical plane that results in opposite strains on each horizontal side. This appears as the red and blue sides as displayed on the right face. In the middle of the slit width the forces cancel each other out as shown as the average green down the center.

There are very few discernable features in Fig. 4, the transverse strain. These results are not surprising considering the mechanical environment of the slit. Remember that the slit was designed to reduce deformation and strain in the transverse direction, originally to reduce out-of-plane effects in 2D imaging. Note that the colormap has the smallest range scale of the three images. There are some somewhat random bright spots on the right face of the cube. It also appears that there is slightly larger strain in the anterior which decreases gradually from anterior to posterior. This is probably related to the larger depth dependence of the vertical strain as there is some interaction between all of the strains.

IV. Discussion

There were three improvements to the methods and setup since previous measurements and reporting [14] on 2-D images of strain obtained with an earlier version of the ultrasound elasticity microscope. The most obvious enhancement was the addition of a third axis which enabled 3-D imaging. Because the same type of deformation plate was used in both cases, the tissue deformed in a similar

manner. As was mentioned earlier the slit was designed to minimize motion out of the 2-D imaging plane. As shown in Fig. 4, three-dimensional imaging does confirm that out-of-plane motion is minimized and gives some confidence to previous 2-D images of strain. However, although minimized, Fig. 4 also confirms that there is some small transverse strain that justifies 3-D imaging even with a slit setup.

The second improvement to the methods was the addition of a reservoir system to maintain physiological pressure in the globe. Previously the eye was inflated with a very thin needle and syringe prior to the experiment but this pressure was not necessarily maintained. There was probably some gradual decrease in the pressure throughout the experiment that may have affected the final results. With the improved pressure system, more confidence can be placed in the results.

Finally, with the new methods, extensive measurements were conducted to reduce the effects of corneal edema. In these preliminary measurements chemical composition was varied until a composition was found that minimized deformation from edema. Deformation from edema probably explains the previously reported 2-D maps of strain. In that case, the epithelial layer showed compressional strain while the stroma indicated expansional strain. Most likely edema rather than external deformation created expansion in the stroma. The rate of edema is such that the stroma probably pulled fluid from the epithelium causing compression. Because of the edema control experiments, we can be confident that the 3-D images of strain are the result of the deformation plate rather than edema.

V. Conclusions

We have shown that an ultrasound elasticity microscope can effectively determine three-dimensional images of strain in a porcine cornea. Three types of directional strain were determined from the data: longitudinal, horizontal, and transverse. Each of these three strains behaved as was expected under the conditions of being deformed by a slitted plate. These measurements are an advancement over the original two-dimensional results. Edema is better controlled, physiologic pressure is better maintained, and out-of-plane motion is tracked.

The next objectives are to calculate mechanical moduli maps from strain data and to apply this technique to *ex vivo* human eye globes. Ultimately, this information should lead to a better understanding of the mechanical property changes leading to keratoconus and better outcomes for corneal refractive surgery.

Acknowledgment

We thank the NIH Resource Center for Medical Ultrasonic Transducer Technology at the University of Southern California for designing and building the high-frequency transducer used in this study.

References

[1] R. Lerner, K. Parker, J. Holen, R. Gramiak, and R. Waag, "Sonoelasticity: medical elasticity images derived from ultrasound signals in mechanically vibrated targets," in *Acoustic Imaging*, vol. 16. New York: Plenum Press, 1988, pp. 317-327.

[2] J. Ophir, I. Cespedes, H. Ponnekanti, Y. Yazdi, and X. Li, "Elastography - a Quantitative Method for Imaging the Elasticity of Biological Tissues," *Ultrasonic Imaging*, vol. 13, pp. 111-134, 1991.

[3] A. R. Skovoroda, S. Y. Emelianov, M. A. Lubinski, A. P. Sarvazyan, and M. Odonnell, "Theoretical-Analysis and Verification of Ultrasound Displacement and Strain Imaging," *IEEE Transactions on Ultrasonics Ferroelectrics and Frequency Control*, vol. 41, pp. 302-313, 1994.

[4] J. Ophir, I. Cespedes, B. Garra, H. Ponnekanti, Y. Huang, and N. Maklad, "Elastography: Ultrasonic imaging of tissue strain and elastic modulus in vivo," *European Journal of Ultrasound*, vol. 3, pp. 49-70, 1996.

[5] T. J. Hall, Y. Zhu, C. S. Spalding, and L. T. Cook, "In vivo results of real-time free hand elasticity imaging," presented at IEEE Ultrasonics Symposium, Atlanta, GA, 2001.

[6] B. J. Geiman, L. N. Bohs, M. E. Anderson, S. M. Breit, and G. E. Trahey, "A novel interpolation strategy for estimating subsample speckle motion," Physics in Medicine and Biology, vol. 45, pp. 1541-1552, 2000.

[7] E. Konofagou and J. Ophir, "A new elastographic method for estimation and imaging of lateral displacements, lateral strains, corrected axial strains and Poisson's ratios in tissues," Ultrasound in Medicine and Biology, vol. 24, pp. 1183-1199, 1998.

[8] P. Chaturvedi, M. F. Insana, and T. J. Hall, "2-D companding for noise reduction in strain imaging," IEEE Transactions on Ultrasonics Ferroelectrics and Frequency Control, vol. 45, pp. 179-191, 1998.

[9] M. A. Lubinski, S. Y. Emelianov, K. R. Raghavan, A. E. Yagle, A. R. Skovoroda, and M. Odonnell, "Lateral displacement estimation using tissue incompressibility," IEEE Transactions on Ultrasonics Ferroelectrics and Frequency Control, vol. 43, pp. 247-256, 1996.

[10] M. A. Lubinski, S. Y. Emelianov, and M. O'Donnell, "Speckle tracking methods for ultrasonic elasticity imaging using short-time correlation," IEEE Transactions on Ultrasonics Ferroelectrics and Frequency Control, vol. 46, pp. 82-96, 1999.

[11] X. Chen, H. Xie, R. Erkamp, K. Kim, C. Jia, J. M. Rubin, and M. O'Donnell, "3-d correlation-based speckle tracking," EnglishUltrasonic Imaging, vol. 27, no. 1, pp. 21–36, 2005.

[12] S. Tripathy, M. A. Simon, and K. Kim, "Quantitative evaluation of correlation-based 3d vs. 2d speckle tracking using finite element cardiac mechanical model and in-vitro phantom." in IEEE International Ultrasonics Symposium, 2010.

[13] S. Tripathy, M. A. Simon, M. S. Sacks, J. C. Brigham, and K. Kim, "3-dimensional ultrasound elasticity imaging for quantitative cardiac mechanical property assessment: a numerical approach," Proceedings of the ASME 2010 Summer Bioengineering Conference, 2010

[14] R. H. Kennedy, W. M. Bourne, and J. A. Dyer, "A 48-Year Clinical and Epidemiologic-Study of Keratoconus," American Journal of Ophthalmology, vol. 101, pp. 267-273, 1986.

[15] N. A. Cohn, S. Y. Emelianov, M. A. Lubinski, and M. O'Donnell, "An Elasticity Microscope. Part I: Methods," *IEEE Trans. Ultrason., Ferroelect., Freq. Contr.*, vol. 44, pp. 1304-1319, 1997.

[16] N. A. Cohn, S. Y. Emelianov, and M. O'Donnell, "An Elasticity Microscope. Part II: Experimental Results," *IEEE Trans. Ultrason., Ferroelect., Freq. Contr.*, vol. 44, pp. 1320-1331, 1997.

[17] K. W. Hollman, S. Y. Emelianov, J. H. Neiss, G. Jotyan, G. J. R. Spooner, T. Juhasz, R. M. Kurtz, and M. O'Donnell, "Strain imaging of corneal tissue with an ultrasound elasticity microscope," *Cornea*, vol. 21, pp. 68-73, 2002.

[18] K. W. Hollman, "Time Progression and Depth Dependence of High Frequency AIBS in *Ex-Vivo* Porcine Corneas", 2010 IEEE Ultrasonics Symposium, San Diego, CA.